Water Research 122 (2017) 355–362

Contents lists available at ScienceDirect

Water Research

journal homepage: www.elsevier.com/locate/watres

The distribution of phosphorus and its transformations during batch growth of *Synechocystis*

Yun Zhou [a, b], Binh T. Nguyen [a], Chen Zhou [a], Levi Straka [a], YenJung Sean Lai [a], Siqing Xia [b, *], Bruce E. Rittmann [a, **]

[a] Biodesign Swette Center for Environmental Biotechnology, Arizona State University, Tempe, AZ 85287-5701, United States
[b] State Key Laboratory of Pollution Control and Resource Reuse, College of Environmental Science and Engineering, Tongji University, Shanghai 200092, China

ARTICLE INFO

Article history:
Received 10 April 2017
Received in revised form
19 May 2017
Accepted 6 June 2017
Available online 9 June 2017

Keywords:
Phosphorus
Cyanobacterium
Extracellular polymeric substances (EPS)
Intracellular phosphorus pool
Transformation pathway

ABSTRACT

Phosphorus (P) is an essential nutrient that affects the growth and metabolism of microalgal biomass. Despite the obvious importance of P, the dynamics of how it is taken up and distributed in microalgae are largely undefined. In this study, we tracked the fate of P during batch growth of the cyanobacterium *Synechocystis* sp. PCC 6803. We determined the distribution of P in intracellular polymeric substances (IPS), extracellular polymeric substances (EPS), and soluble microbial products (SMP) for three initial ortho-phosphate concentrations. Results show that the initial P concentration had no impact on the production of biomass, SMP, and EPS. While the initial P concentration affected the rate and the timing of how P was transformed among internal and external forms of inorganic P (IP) and organic P (OP), the trends were the same no matter the starting P concentration. Initially, IP in the bulk solution was rapidly and simultaneously adsorbed by EPS (IP_{EPS}) and taken up as internal IP (IP_{int}). As the bulk-solution's IP was depleted, desorption of IP_{EPS} became the predominant source for IP that was taken up by the growing cells and converted into OP_{int}. At the end of the 9-d batch experiments, almost all P was OP, and most of the OP was intracellular. Based on all of the results, we propose a set of transformation pathways for P during the growth of *Synechocystis*. Key is that EPS and intracellular P pool play important and distinct roles in the uptake and storage of P.

1. Introduction

Fossil fuels provide at least 80% of energy demand worldwide (Goldemberg et al., 2004), but the combustion of fossil fuels is increasing the concentration of atmospheric CO_2, resulting in global warming and climate change (Rittmann, 2008). Photosynthesis captures photons from sunlight, takes up CO_2, and generates plant, algae, and cyanobacterial biomass (Kim et al., 2011b; Rittmann, 2008; Rittmann et al., 2006). Since its lipid portion can be converted to biodiesel and the non-lipid proportions can be used to produce methane, hydrogen and electricity (Chisti, 2007; Kim et al., 2011a; Rittmann, 2008), cyanobacterial has been studied extensively in recent decades.

Among the factors that affect the growth of cyanobacterial biomass, phosphorus (P) is an important nutrient that regulates growth and metabolism (Borovec et al., 2010; Theodorou et al., 1991; Zevin et al., 2015). At the metabolic level, many studies have focused on the effect of P on the activity of extracellular phosphatases, the P-uptake rate, and the role of P in controlling the rate of photosynthesis (Fredeen et al., 1990; Goldstein et al., 1989; Huang et al., 2015; Lefebvre et al., 1990; Rivkin and Swift, 1985; Yao et al., 2011). For example, low-P may diminish ribulose-1,5-bis-phosphate (RuBP) regeneration and, hence, photosynthetic CO_2-fixation by reducing Calvin-cycle enzyme activity (Fredeen

Abbreviations: P, Phosphorus; IP, inorganic phosphorus; OP, organic phosphorus; TP, total phosphorus; BS, bulk solution; EPS, extracellular polymeric substances; IPS, intracellular polymeric substances; SMP, soluble microbial products; IP_{EPS}, inorganic P in EPS; IP_{BS}, inorganic P in the bulk solution; IP_{int}, intracellular inorganic P; OP_{SMP}, OP in SMP; OP_{EPS}, OP in EPS; OP_{int}, intracellular OP; PG, phosphatidylgcerol; ADP, adenosinediphosphate; ATP, adenosinetriphosphate; OD, optical density; DW, dry weight; PCOD, particulate chemical oxygen demand; SCOD, soluble chemical oxygen demand; BSA, bovine serum albumin.

* Corresponding author.
** Corresponding author.
E-mail addresses: siqingxia@tongji.edu.cn (S. Xia), Rittmann@asu.edu (B.E. Rittmann).

http://dx.doi.org/10.1016/j.watres.2017.06.017
0043-1354/

et al., 1990). Understanding the effect of P distribution on the growth rate of microalgae will be of value for stimulating microalgae growth in cultures used for biofuel production and other valuable products and for minimizing their undesired growth in water bodies.

Total P in aquatic systems consists of inorganic phosphate (IP) and P-containing organic compounds (OP) (Francko and Heath, 1979), both of which can be further partitioned into an extracellular P pool (P not inside microorganisms) and an intracellular P pool (P inside microorganisms) (Cembella et al., 1984; Yao et al., 2011). The uptake of inorganic P (IP) by biomass also involves its adsorption by extracellular polymeric substances (EPS), a process that is distinct from and independent of its uptake as intracellular P (Yao et al., 2011; Zhang et al., 2013). EPS are microbe-produced solids that are located outside the cell and are comprised of protein, carbohydrate, and other organic components (Adav and Lee, 2008). A common functional group in protein, quaternary ammonium ($-NH_3^+$), can complex with negatively charged phosphate (Wingender et al., 1999; Zhou et al., 2017). For example, when the pH was greater than 8, the key surface ligand for the EPS of *Shewanella alga* strain BrY was $-NH_3^+$ (Deo et al., 2010). EPS-adsorbed P was 60–90% of total cellular P in different algal species (Sañudo-Wilhelmy et al., 2004).

Within the cells, IP from the bulk solution (IP_{BS}) can be transported across the cellular membrane and become part of intracellular IP (IP_{int}) (Cembella et al., 1984). Part of IP_{int} is IP that is adsorbed by the $-NH_3^+$ groups of organic components in intracellular polymeric substances (IPS) (Deo et al., 2010). Another part of IP_{int} is non-adsorbed IP that participates in conversion of adenosinediphosphate (ADP) to adenosinetriphosphate (ATP) (Novikoff et al., 1952). IP_{int} can be transformed into intracellular OP (OP_{int}) during biomass synthesis (Kim et al., 2011b).

Fig. 1 illustrates and defines the locations in which IP and OP exist in cyanobacterial biomass or the liquid medium. The biomass contains EPS and IPS, which are located outside and inside the cell membrane, respectively (Adav and Lee, 2008). SMP are soluble cellular components that are released from the biomass (Wingender et al., 1999). IP can be free or adsorbed. Free IP exists dissolved in the bulk solution (IP_{BS}) and inside the cell (IP_{int}), such as for use to convert ADP to ATP (Novikoff et al., 1952). Adsorbed IP is present in SMP, EPS, and IPS due to it complexation with $-NH_3^+$ functional groups (Deo et al., 2010). P in nucleic acids and lipids is part of OP, and it can be found in soluble microbial product (SMP), EPS and intracellular P pool (Youngburg and Youngburg, 1930).

Despite the obvious importance of P partitioning and transformation, little is known about these factors during the growth of microalgae. In this study, we carried out batch growth experiments with *Synechocystis* sp. PCC 6803, a well characterized cyanobacterium that has been widely used as a model organism in a variety of molecular and engineering studies (Kim et al., 2011b; Zevin et al., 2015). Establishing a complete P mass balance, we systematically investigated how added inorganic phosphate was transformed and distributed among the IP and OP components as *Synechocystis* grew in batch culture. No matter the staring P concentration, sorption of IP was the dominant mechanism at the beginning of batch-growth studies, but most P was transformed to OP by the end of the batch growth. We translate the results into a model for the dynamics of P uptake and distribution.

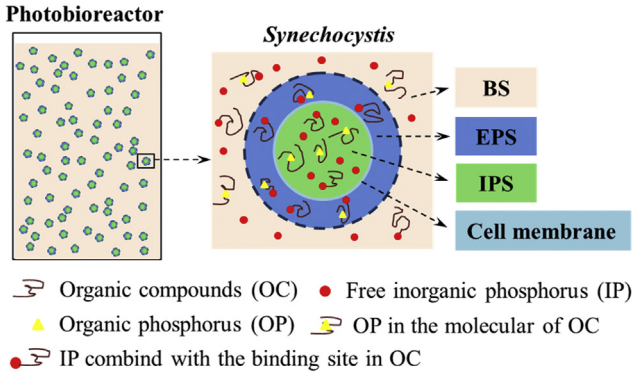

Fig. 1. Definitions of the various forms of inorganic and organic P among the components of *Synechocystis*.

2. Materials and methods

2.1. Synechocystis sp. PCC 6803 cultures and growth experiments

Stock cultures of wild-type *Synechocystis* sp. PCC 6803, provided by the laboratory of Dr. Willem F. J. Vermaas (School of Life Sciences, Arizona State University), were maintained in 500-mL (working volume) Erlenmeyer flasks containing standard BG-11 medium (Rippka et al., 1979) (composition in Table S1) and bubbled with air filtered through a 1.0-μm air filter (Pall, Port Washington, NY, U.S.). An aliquot from a flask culture was diluted to an optical density (OD) of ~0.6 to initiate a batch growth experiments. Table 1 summarizes characteristics of the *Synechocystis* inoculate at the start of batch experiments.

Erlenmeyer flasks with a volume of 1000 mL were used for batch growth experiments. A constant temperature of 30 °C was maintained by 3 × 12-W automated-air fans (Minebea-Matsushita Motor Corp., Japan) (Nguyen and Rittmann, 2016a), and pure CO_2 was supplied by sparging with humidified air filtered through the 1.0-μm air filter (Pall, Port Washington, NY, USA). The incident light intensity was 276 μE/m^2/s, measured using a PAR sensor (Agilent, U1252A, USA), and it was provided from T5 fluorescent plant-grow lamps (Envirogro Hydrofarm, USA). The pH value of the culture was maintained at 8.5 using a pH-Stat that automatically sparged CO_2 when the pH rose above 8.51 (Nguyen and Rittmann, 2015). Fig. S1 is a schematic diagram of the set up for the growth experiments.

Previous study (Kim et al., 2011b) measured the elemental composition of *Synechocystis* sp. PCC 6803 and found it to be

Table 1
Characteristics of the *Synechocystis* inoculum used to initiate growth experiments.

Parameter	Value
OD_{730}[a]	0.59 ± 0.04
PCOD[b] (mg COD/L)	250 ± 11
SMP[c] (mg COD/L)	6.3 ± 0.45
EPS[d] (mg COD/L)	14.8 ± 0.38
Protein in SMP (mg COD/L)	1.68 ± 0.21
Carbohydrate in SMP (mg COD/L)	3.68 ± 0.49
Protein in EPS (mg COD/L)	8.47 ± 0.39
Carbohydrate in EPS (mg COD/L)	5.32 ± 0.42
IP[e] in SMP (mg P/L)	0.078 ± 0.011
OP[f] in SMP (mg P/L)	0.032 ± 0.007
IP in EPS (mg P/L)	0.141 ± 0.028
OP in EPS (mg P/L)	0.093 ± 0.006
IP in IPS (mg P/L)	0.062 ± 0.010
OP in IPS (mg P/L)	0.335 ± 0.031
TP[g] of *Synechocystis* (mg P/L)	0.752 ± 0.079

[a] OD_{730} is the optical density at 730 nm.
[b] PCOD is particulate chemical oxygen demand.
[c] SMP is soluble microbial products.
[d] EPS is extracellular polymeric substances.
[e] IP is inorganic phosphorus.
[f] OP is organic phosphorus.
[g] TP is total phosphorus.

$C_{1.00}H_{1.62}O_{0.40}N_{0.22}P_{0.01}$. Because the mole ratio of N:P in standard BG-11 medium is 101:1,[28] which has far higher N than needed by stoichiometry (22:1), we decreased the NO_3-N concentration to 120 mg N/L (8.6 mM) and increased the P concentration to 12 mg P/L (0.39 mM) as baseline concentrations consistent with the stoichometric ratio of 22 mol N/mol P. To evaluate the effects of P limitation, we used three starting concentrations of P (mM): 0.39 (experiment R1), 0.16 (R2) and 0.055 (R3). We prepared the P stock solution by dissolving K_2HPO_4 in distilled water at an initial concentration of 5.4 g P/L (174 mM). We also augmented the starting alkalinity by adding 6.0 mM of bicarbonate (as $NaHCO_3$). All constituents other than N, P, and alkalinity were the same as standard BG-11 (Rippka et al., 1979). The volume of the culture was 700 mL. Prior to inoculation, the flasks and the BG-11 medium were sterilized by autoclaving, and the pH probe was sterilized using 75% ethanol. For each starting concentration, we conducted three independent experiments.

2.2. Phosphorus distribution

Fig. 2 illustrates the centrifugation- and thermal-based method used to separate SMP, EPS, and IPS from *Synechocystis* cells. We first centrifuged a sample at 4000 rpm and 4 °C for 15 min and further centrifuged the supernatant at 12,000 rpm (Microfuge® 22R Centrifuge, Beckman Coulter, CA, USA) and 4 °C for 10 min to remove all particles. We then collected the supernatant (denoted s1), which contained the SMP. We collected the pellets after both centrifugations and resuspended them to their original volumes using the pH-8.4 borate buffer, which consists of 0.49 mM H_3BO_3 and 0.2 mM $Na_2B4O_7 \cdot 10H_2O$ (Wang et al., 2017). The suspensions were heating at 60 °C for 20 min and then centrifuged at 4000 rpm at 4 °C for 15 min (Zhou et al., 2016a,b). The supernatant was further centrifuged at 12,000 rpm at 4 °C for 10 min to remove all particles, and the collected supernatant (denoted s2) contained the EPS. We collected the pellets from the EPS extraction and resuspended them to their original volumes using borate buffer; this suspension contained the IPS. In order to destroy the cell membrane completely, we heated this suspension in a boiling-water bath for 60 min (temperature about 100 °C), centrifuged the suspension at 12,000 rpm at 4 °C for 10 min, and collected the supernatant (denoted s3). With the components of phospholipids and glycoproteins, cell membrane also contains OP (Youngburg and Youngburg, 1930). As cell membrane and IPS were mixed in the boiling-water bath, intracellular OP (OP_{int}) contains OP in both cell membrane and IPS. All of the supernatants (s1, s2, and s3) and IPS suspension were stored at 4 °C in a freezer (UGL3020A, Thermo Scientific, USA) prior to all analyses.

2.3. Analytical methods

We measured the Optical Density (OD) of the culture using a UV–vis BioSpec-mini spectrometer at 730 nm (Shimadzu Corp., Japan). We determined the dry weight (DW) of biomass using total suspended solids, assayed by Method 2540D in *Standard Methods* (Association, 1998), and DW was converted to particulate chemical oxygen demand (PCOD) using 1.4 mg COD/mg DW (Rittmann and McCarty, 2001). We measured total phosphorus (TP) and reactive phosphate using the HACH TNT843 kit. The reactive phosphate was the IP, and the OP was equal to the TP minus IP. We measured NO-3using a HACH TNT880 kit (Loveland, CO, USA). We measured the soluble chemical oxygen demand (SCOD) of SMP and EPS using HACH TNT822 kits (0–60 mg/L). All HACH test vials were treated according to the manufacturer's instruction and analyzed in a HACH DR 2800 spectrophotometer.

We measured the protein fraction of SMP and EPS with a QuantiPro BCA Assay Kit (Sigma-Aldrich, St. Louis, MO, U.S.) using bovine serum albumin (BSA) as the standard; BSA equivalents were converted to COD using a conversion factor of 1.4 mg COD/mg BSA (Rittmann and McCarty, 2001). We measured the carbohydrate fraction of SMP and EPS with the phenol-sulfuric acid method using glucose as the standard (Chojnacka and Noworyta, 2004) and converted glucose equivalents to COD using a conversion factor of 1.07 mg COD/mg glucose (Rittmann and McCarty, 2001).

2.4. Statistical analyses

We carried out triplicate separations of SMP, EPS, and IPS, and each sample was assayed one time for DW, SCOD, IP, TP, NO_3^-, protein and carbohydrate. Results are expressed as the mean and standard deviation of the three measured samples (mean ± SD).

3. Results and discussion

3.1. Production of biomass, SMP, and EPS

Fig. 3 shows the concentrations of residual IP_{BS}, biomass, SMP, EPS, protein, and carbohydrate in SMP and EPS for the batch experiments with the three starting P concentrations. We present one set of results for each concentration. The results for the two replicate runs for each starting-P concentration were similar and are

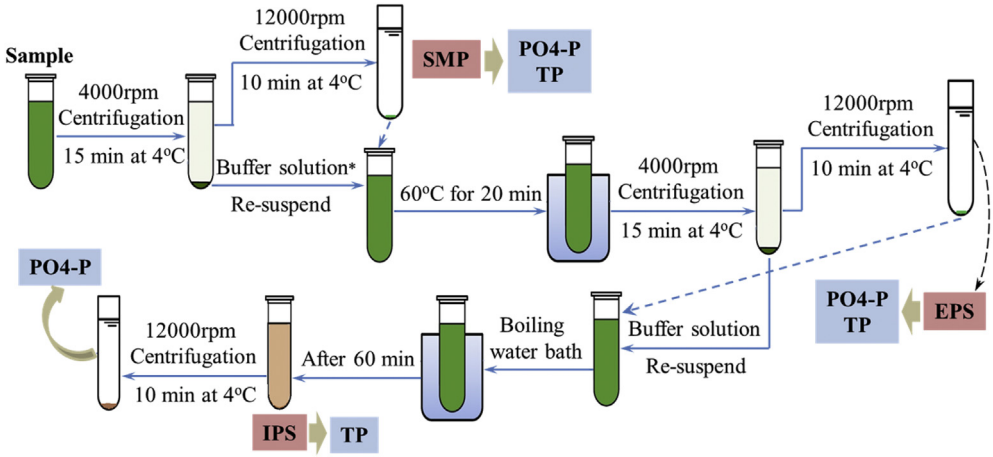

Fig. 2. The centrifugation- and thermal-based extraction protocol for the separation of SMP, EPS, and IPS in *Synechocystis*.

summarized in Figs. S2–S3 in the SI. Starting P made little difference for the concentrations of biomass (denoted PCOD for the total particulate COD), SMP, EPS, protein and carbohydrate in SMP and EPS. Likewise, the utilization of NO_3^--N was almost the same (Fig. S6). PCOD rapidly increased from 1 d to 4 d, and then it slowly increased; the slowdown in growth rate resulted from the decrease of average light intensity and specific growth rate with increasing biomass concentration (Fig. S7), making light limitation significant in the later stages of the experiment. The most important conclusion from Fig. 3 is that *Synechocystis* grew normally and equally with the different initial P concentrations.

The growth of biomass was independent of the depletion of inorganic P in the bulk solution. IP_{BS} approached zero concentration as early as 2 d for R3, although full depletion took 9 d for R1. Thus, *Synechocystis* continued to grow well whether or not IP_{BS} was available.

EPS accumulation mirrored PCOD with a lag of about 1 d, while SMP increased more steadily (Fig. 3(b)). *Synechocystis* produced more EPS than SMP, but the gap narrowed with increasing incubation time, since hydrolysis of EPS is a major source of SMP (Laspidou and Rittmann, 2002). Accumulations of protein and carbohydrate in SMP and EPS mirrored the increases of SMP and EPS. The concentration of carbohydrate was higher than protein in SMP, but the opposite was true for EPS, a trend that is consistent with a previous study (Ramesh et al., 2006) that indicated that proteins accumulate in EPS, while carbohydrates become predominant in SMP.

At the end of the batch experiments, SMP and EPS corresponded approximately to 7.5% and 8.4% of PCOD, respectively. Previous studies (Ge et al., 2014; Nguyen and Rittmann, 2016b) also noted that phototrophic cells began to produce significant amounts of SMP during growth, but they did not measure EPS. The cyanobacterium *Microcoleus vaginatus* exposed to 40 and 80 $\mu E/m^2/s$ produced SMP at 8.0% and 14% of cell DW, respectively (Ge et al., 2014). SMP was about 18% of TCOD for wild-type *Synechocystis* exposed to 598 $\mu E/m^2/s$ for 8 days (Nguyen and Rittmann, 2016b). A possible trend among these studies is that higher light intensity led to greater SMP production (Nguyen and Rittmann, 2016b).

3.2. Distribution of phosphorus

Fig. 4 presents the distributions of IP and OP in all of the components of *Synechocystis* during the batch experiments. Again, the results for the two replicate runs were similar, and they are summarized in Figs. S4–S5 in the SI. The excellent P mass balance (<2.5% discrepancy) in the batch experiments indicates the effectiveness of the extraction and determination methods. IP_{BS} in all of the experiments dropped rapidly and virtually disappeared, although higher initial P concentration needed a longer time for depletion. IP_{BS} was most immediately replaced by intracellular P (P_{int}); thus, initial P-uptake involved significant uptake and accumulation of IP_{int}.

Another significant part of the lost IP_{BS} was IP held in EPS. Although IP_{EPS} increased more slowly than IP_{int} in the first hours of the experiments, it became an important sink of IP (>68%) as IP_{BS} was nearly depleted. IP_{EPS} decreased after IP_{BS} was depleted, which suggests that IP_{EPS} became an important supply of IP for biomass growth once IP_{BS} was depleted.

Later in the experiments, IP was transformed to OP. Whereas IP_{int} was much greater than OP_{int} in the early stages of the experiments, IP_{int} subsequently began to decrease as OP_{int} increased. Most intercellular P was OP_{int} at the end of the 9-day experiments. Likewise, OP_{EPS} gradually gained importance as IP_{BS} and IP_{EPS} were depleted. The last P component to become significant was OP_{SMP}, which gradually increased in parallel with the steady increase of SMP (Fig. 3(b)). A previous study (Nguyen and Rittmann, 2016b) found that SMP was about 18% of total COD for wild-type *Synechocystis* after 8 days of batch growth, which supports that SMP should be an important extracellular sink of OP, perhaps due to its content of nucleic acids and lipids (Youngburg and Youngburg, 1930).

By the end of the batch experiments, almost all P was OP, and most of the OP was OP_{int}. Reducing the starting P concentration shorted the time needed for IP to be transformed to OP and

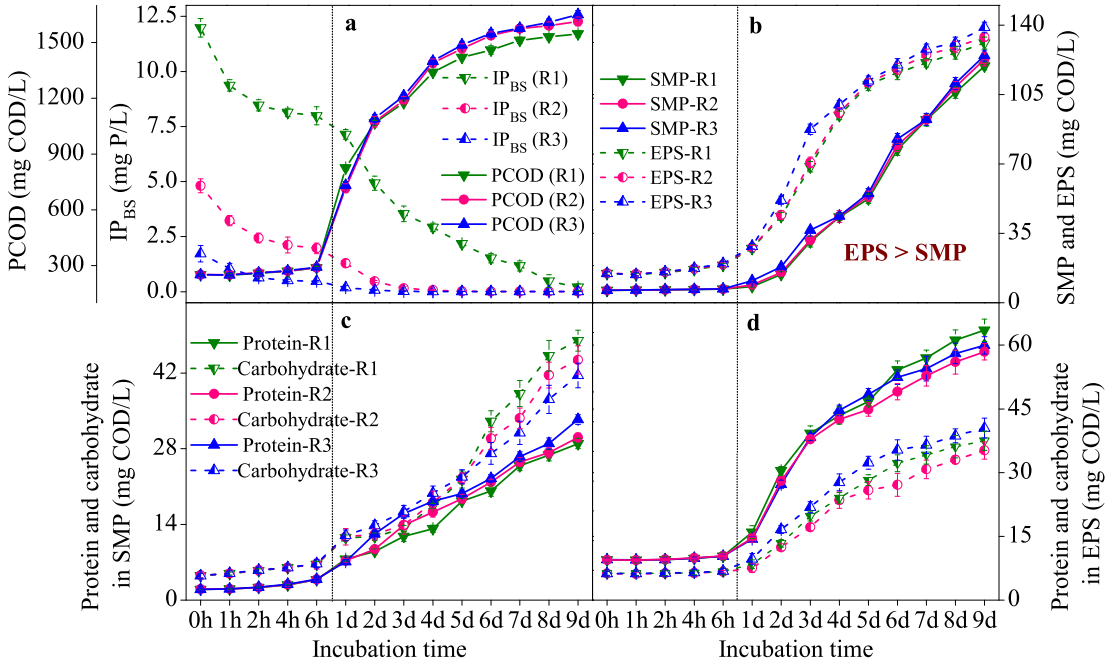

Fig. 3. Concentration of (a) total biomass (PCOD) and residual IP_{BS}, (b) SMP and EPS, (c) protein and carbohydrate in SMP, and (d) protein and carbohydrate in EPS for the three initial P concentrations for the batch growth experiments. Note that the time scale is not linear.

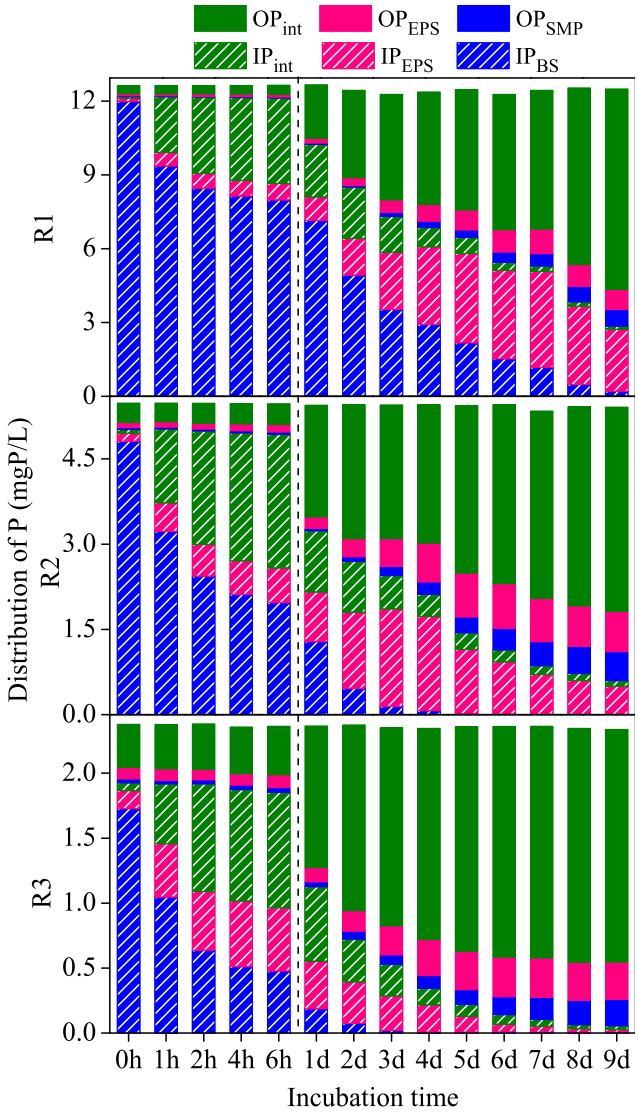

Fig. 4. Distribution of P for the three starting P concentrations at the noted incubation times. Note that the time scale in not linear.

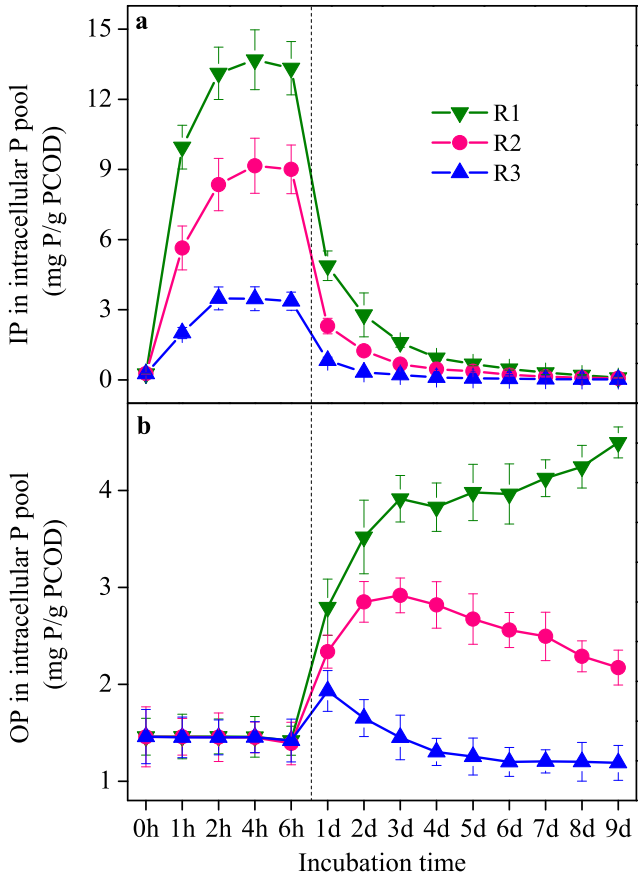

Fig. 5. IP and OP in the intracellular phosphorus pool of *Synechocystis* for the three starting P concentrations at the noted incubation times. Note that the time scale is not linear.

especially OP_{int} (Table S2).

3.3. IP_{int} and OP_{int} in the intracellular P pool of Synechocystis

Fig. 5 shows the IP_{int} and OP_{int} contents in the intracellular P pool of *Synechocystis* for the batch experiments. IP_{int} rapidly increased and reached its maximum values after 4 h; the transfer occurred sooner with a higher starting P concentration, which also resulted to a higher maximum IP_{int}. The transport rate of IP from BS to intracellular P pool is related to the IP concentration in BS and the intracellular P pool (Armstrong, 2008): High IP_{BS} and low IP_{int} in *Synechocystis* in the initial stage (Fig. 4) increased the IP-transport rate and the consequent accumulation of IP in the intracellular P pool. During the rapid-uptake phase, intracellular P pool contained 54%–84% of total cellular P (Fig. S8). Later, the OP_{int} converted from IP_{int} continued to accumulate in the biomass for the experiment with the highest starting P concentration, but it decreased after a brief increase in the experiment with the lowest starting P concentration. Thus, the intracellular P pool quickly captured IP, which was subsequently converted into OP during the synthesis of *Synechocystis* biomass. *Synechocystis* synthesized new cells with low OP_{int} content when the starting P concentration was low.

3.4. IP and OP in the EPS of Synechocystis

Fig. 6 shows the contents of IP and OP in the EPS of *Synechocystis* for the three batch experiments. IP_{EPS} dramatically increased and reached the maximum value after 2 h, and increasing the starting P concentration led to more IP_{EPS}, which is consistent with the sorption being the mechanism for formation of IP_{EPS} (Zhang et al., 2014). The uptake rate was faster with a higher starting P concentration, which is consistent the uptake rate being positively correlated with the concentration of nutrient in BS (Rivkin and Swift, 1985). The functional group for sorption is the $-NH_3^+$ group, which mainly exists in protein (Deo et al., 2010; Zhou et al., 2017) and Fig. 7(a) shows a strong and nearly linear relationship ($R^2 = 0.955$, $P = 0.00$) between the contents of IP_{EPS} and protein in EPS. In contrast, the linear regression between the contents of IP_{EPS} and carbohydrate in EPS is not significant ($R^2 = 0.515$, $P = 0.10$). Later in the experiments, the protein proportion in EPS remained almost stable (Fig. S9), and the decrease of IP_{EPS} probably as the result of net desorption of IP_{EPS} from the protein. The decrease of IP_{EPS} lagged behind decrease of IP_{BS}, which underscores that IP_{EPS} was a significant storage pool for IP.

OP_{EPS} rapidly increased and then remained stable in the reactor with high starting P concentration. However, OP_{EPS} had only a brief increase, and its rapid decrease occurred sooner in the reactor with low starting P concentration. Later in the experiments, OP_{EPS} gradually decreased, even though EPS dramatically increased and

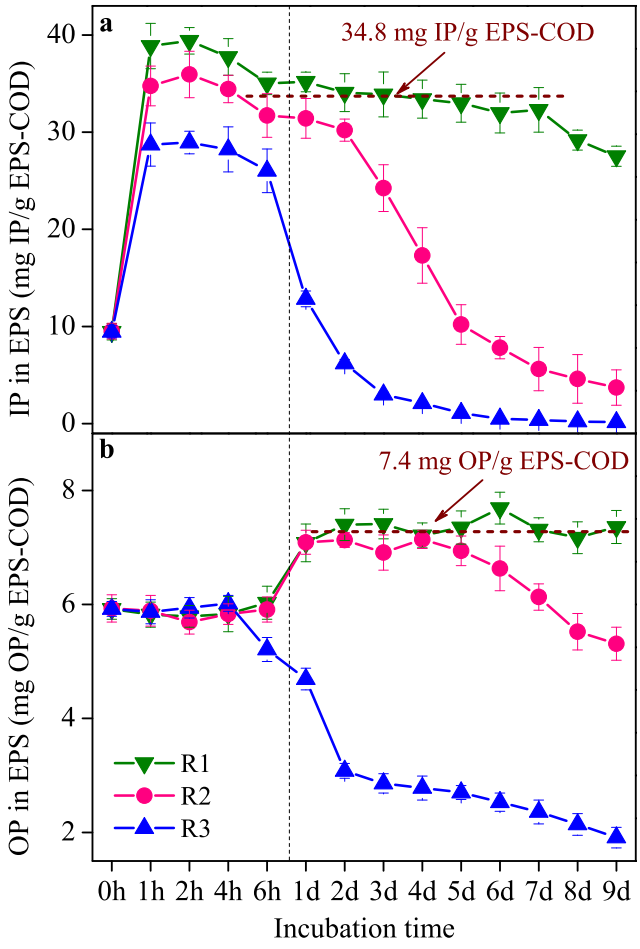

Fig. 6. (a) IP and (b) OP in the EPS of *Synechocystis* for the three experiments at the noted incubation times. Note that the time scale is not linear.

the total concentration of OP_{EPS} slightly increased (Figs. 3 and 4). Thus, *Synechocystis* secreted EPS with low OP content when IP_{int} and IP_{EPS} dramatically decreased and even depleted in the later stage due to cell growth.

EPS was an important part of the P pool, containing 16%–46% of total cellular P (Fig. S8). When IP_{BS} was plentiful, EPS rapidly adsorbed IP from BS, giving a high P content in the EPS. As IP_{BS} was depleted, IP_{EPS} desorption became the main source of IP_{BS}.

3.5. OP in the SMP of Synechocystis

Fig. 8 shows the content of OP in the SMP of *Synechocystis* for the three batch experiments. OP_{SMP} in R1-R3 gradually increased in the initial 6 h at an approximately linear rate of 0.022 mgP/(gSMP-COD·h). In the reactor with the highest initial P concentration, OP_{SMP} keep increasing from 6 h to 3 d and then remained stable from 3 d to 7 d, but gradually increased again later. OP_{EPS} remained stable from 7 d to 9 d, while OP_{int} content gradually increased in this stage. Thus, OP_{int} converted into OP_{SMP}, which is consistent with biomass producing utilization-associated products (UAP) as part of SMP (Laspidou and Rittmann, 2002). In the reactor with low starting P concentration, OP_{SMP} showed only a slight increase in the initial several hours, and the rapid decrease occurred sooner, even though the SMP content dramatically increased (Fig. 3). Thus, *Synechocystis* produced SMP with low OP content when IP_{int} and IP_{EPS} dramatically decreased and even became depleted in the later stage of the experiment.

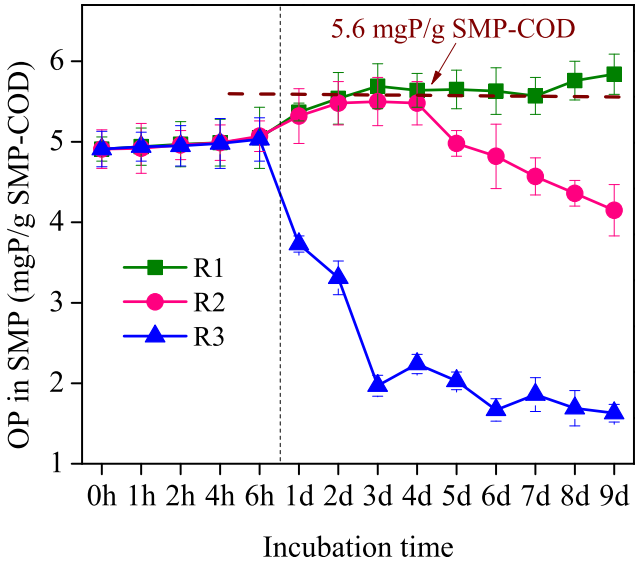

Fig. 8. OP in the SMP of *Synechocystis* for the three experiments at the noted incubation times. Note that the time scale is not linear.

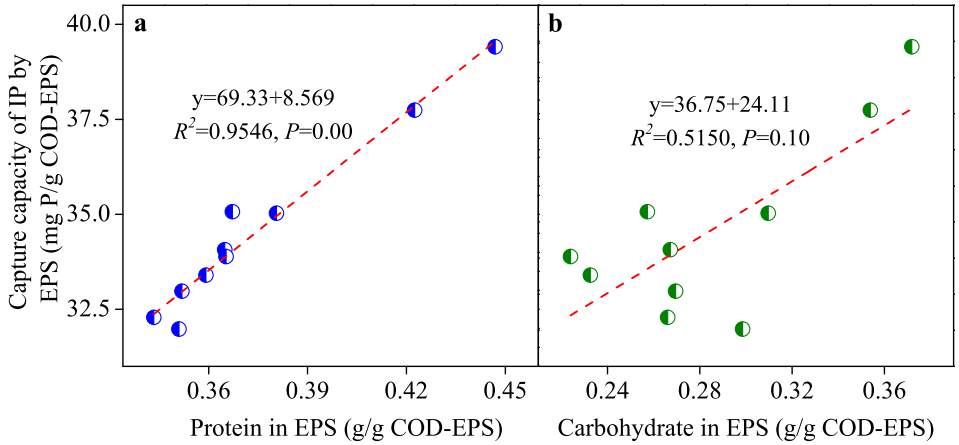

Fig. 7. The relationship between the content of IP_{EPS} and the proportion EPS that is (a) protein and (b) carbohydrate for the input P concentration of 12.0 mg/L (R1) and with incubation times from 2 h to 7 d. Note that the time scale is not linear.

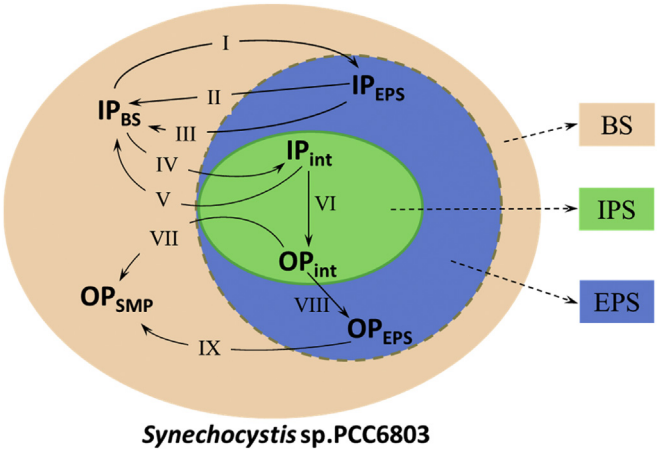

Fig. 9. Proposed model of P-uptake and -transformation processes during the growth of *Synechocystis*. Initially, IP_{BS} is rapidly sorbed by EPS (process I) and taken up as IP_{int} (process IV). As IP_{BS} became depleted, desorption of IP_{EPS} (process II) became the predominant source for IP_{int} taken up, and other part of IP_{EPS} was released to BS (IP_{BS}) during EPS hydrolyzation (process III). Part of IP_{int} was converted into OP_{int} by the growing cells (process VI) and released to BS (IP_{BS}) due to cell decay (process V). Part of OP_{int} was released as OP_{SMP} (process VII) and OP_{EPS} (process VIII), and OP_{EPS} also could be converted to OP_{SMP} (process IX).

3.6. Transformation pathway of P during the growth of *Synechocystis*

Fig. 9 summarizes a model of the transformation routes indicated by the results of the batch experiments. Initially, IP_{BS} was rapidly adsorbed by EPS (process I) and taken up as IP_{int} (process IV). As IP_{BS} became depleted, desorption of IP_{EPS} (process II) became the predominant source for IP_{int} taken up, and another part of IP_{EPS} was released to the bulk solution (IP_{BS}) during EPS hydrolysis (process III). Part of IP_{int} was converted into OP_{int} by the growing cells (process VI) and released as IP_{BS} due to cell decay (process V). Part of OP_{int} was released as OP_{SMP} (process VII) and OP_{EPS} (process VIII), and OP_{EPS} also could be converted to OP_{SMP} (process IX). At the end of the 9-d batch experiments, almost all P was OP, and most of the OP was in intracellular P pool. A previous study (Zhang et al., 2013) also proposed a P-metabolic model for enhanced biological phosphorus removal. However, this model is for very different bacteria in a non-photosynthetic system. Furthermore, their metabolic model does not contain phosphorus-associated processes that we know are important in our study: OP_{EPS} and OP_{int} release into the BS, release of OP in SMP (OP_{SMP}), and IP release due to its desorption from EPS and internal complexes. We clearly show that total P consisted of species of inorganic phosphate (IP) and P-containing organic compounds (OP), and we proposed a much more comprehensive P metabolic model based on a complete P mass balance.

The model and the experimental results upon which the model is based make it clear that EPS and intracellular P pool play key roles in the dynamics of P uptake and transformations in *Synechocystis*. Thus, additional research is needed to define better and to quantify the processes involving EPS and intracellular P pool in P dynamics. High benefit would come from developing and parameterizing a mathematical manifestation of the model in Fig. 9, determining how low-P-stress affects the P-transformation pathways and ascertaining if and how OP_{SMP} and OP_{EPS} are utilized in a P-famine condition.

3.7. Environmental implications

Phosphorus is an important nutrient that regulates growth and metabolism. Our study revealed that EPS and intracellular pools of P pool play important and distinct roles in the uptake and storage of P. The proposed model helps to explain a commonly observed phenomenon (Kim et al., 2011b) and we also observed here: continuing growth of microalgae even when the IP in the medium is totally depleted. Understanding these mechanisms of P of uptake and transformation is important for improving performance when producing microalgal biofuel and for controlling eutrophication in water bodies. EPS exist in all species of microbes, and P is an important nutrient for the growth of microbes; thus, the P-transformation pathways in this study should apply to other microbes.

The fact that ortho-phosphate is rapidly taken up and stored by EPS and internal pools means that the concentration of ortho-phosphate is not a reliable tool for controlling the growth of microalgae, such as *Synechocystis*. Whether the goal is to stimulate microalgae growth in cultures used for producing biofuels and other valuable products and for minimizing their undesired growth in water bodies, measuring inorganic P in the bulk solution is misleading, because the primary sinks for inorganic P are in EPS and internal pools. A total mass balance on IP and OP is needed to assess whether or not microalgal growth is or is not P limited.

4. Conclusion

Investigating the uptake and distribution of P during batch growth of *Synechocystis*, we found that the initial P concentration had almost no impact on the concentrations of biomass, SMP, and EPS. Biomass continued to grow normally after ortho-phosphate in the liquid was completely depleted. While the initial P concentration affected the timing of how P was distributed, it did not alter the transformation steps or the ultimate distribution of P. Initially, IP in the bulk solution was rapidly and simultaneously adsorbed by EPS and taken up as internal IP. As the bulk-solution's IP was depleted, desorption of IP in EPS became the predominant source for IP that was taken up by the growing cells and converted into intracellular OP. At the end of the 9-d batch experiments, almost all P was organic P, and most of that was intracellular. Based on all of the results, we propose a set of transformation pathways for P during the growth of *Synechocystis*. Key is that EPS and intracellular pools of P pool play important and distinct roles in the uptake and storage of P.

Acknowledgments

This work was supported in part by the China Scholarship Council (NO. 201506260022), and the National Science Foundation of China (51678422, 51378368). We thank Dr. Everett Eustance and Megha Patel for valuable contributions to the experimental design, setup and data analysis.

Appendix A. Supplementary data

Supplementary data related to this article can be found at http://dx.doi.org/10.1016/j.watres.2017.06.017.

References

Adav, S.S., Lee, D.-J., 2008. Extraction of extracellular polymeric substances from aerobic granule with compact interior structure. J. Hazard. Mater. 154 (1), 1120–1126.
Armstrong, R.A., 2008. Nutrient uptake rate as a function of cell size and surface transporter density: a Michaelis-like approximation to the model of Pasciak and Gavis. Deep-Sea. Res. Pt. I 55 (10), 1311–1317.
Association, A.P.H., 1998. Standard Methods for the Examination of Water and Wastewater. American Public Health Association, Washington, DC, p. 1268.
Borovec, J., Sirová, D., Mošnerová, P., Rejmánková, E., Vrba, J., 2010. Spatial and temporal changes in phosphorus partitioning within a freshwater cyanobacterial mat community. Biogeochemistry 101 (1–3), 323–333.

Cembella, A.D., Antia, N.J., Harrison, P.J., Rhee, G.Y., 1984. The utilization of inorganic and organic phosphorous compounds as nutrients by eukaryotic microalgae: a multidisciplinary perspective: part 2. CRC. Crit. Rev. Microbiol. 11 (1), 13–81.
Chisti, Y., 2007. Biodiesel from microalgae. Biotechnol. Adv. 25 (3), 294–306.
Chojnacka, K., Noworyta, A., 2004. Evaluation of Spirulina sp. growth in photoautotrophic, heterotrophic and mixotrophic cultures. Enzyme. Microb. Tech. 34 (5), 461–465.
Deo, R.P., Songkasiri, W., Rittmann, B.E., Reed, D.T., 2010. Surface complexation of neptunium (V) onto whole cells and cell components of Shewanella alga: modeling and experimental study. Environ. Sci. Technol. 44 (13), 4930–4935.
Francko, D.A., Heath, R.T., 1979. Functionally distinct classes of complex phosphorus compounds in lake water. Limnol. Oceanogr. 24 (3), 463–473.
Fredeen, A.L., Raab, T.K., Rao, I.M., Terry, N., 1990. Effects of phosphorus nutrition on photosynthesis in Glycine max (L.) Merr. Planta 181 (3), 399–405.
Ge, H., Zhang, J., Zhou, X., Xia, L., Hu, C., 2014. Effects of light intensity on components and topographical structures of extracellular polymeric substances from Microcoleus vaginatus (Cyanophyceae). Phycologia 53 (2), 167–173.
Goldemberg, J., Johansson, T.B., Anderson, D., 2004. World energy assessment: overview: 2004 update. U. N. Dev. Programme.
Goldstein, A.H., Mayfield, S.D., McDaniel, R.G., 1989. Phosphate starvation inducible metabolism in lesculeutum. III. Protein secretion by suspension cultured cells. Plant. Physiol. 91, 175–182.
Huang, W., Huang, W., Li, H., Lei, Z., Zhang, Z., Tay, J.H., Lee, D.-J., 2015. Species and distribution of inorganic and organic phosphorus in enhanced phosphorus removal aerobic granular sludge. Bioresour. Technol. 193, 549–552.
Kim, H.W., Marcus, A.K., Shin, J.H., Rittmann, B.E., 2011a. Advanced control for photoautotrophic growth and CO2-utilization efficiency using a membrane carbonation photobioreactor (MCPBR). Environ. Sci. Technol. 45 (11), 5032–5038.
Kim, H.W., Vannela, R., Zhou, C., Rittmann, B.E., 2011b. Nutrient acquisition and limitation for the photoautotrophic growth of Synechocystis sp. PCC6803 as a renewable biomass source. Biotechnol. Bioeng. 108 (2), 277–285.
Laspidou, C.S., Rittmann, B.E., 2002. A unified theory for extracellular polymeric substances, soluble microbial products, and active and inert biomass. Water. Res. 36 (11), 2711–2720.
Lefebvre, D.D., Duff, S.M.G., Fife, C.A., Julien-Inalsingh, C., Plaxton, W.C., 1990. Response to phosphate deprivation in Brassica nigra suspension cells Enhancement of intracellular, cell surface, and secreted phosphatase activities compared to increases in Pi-absorption rate. Plant. Physiol. 93 (2), 504–511.
Nguyen, B.T., Rittmann, B.E., 2016a. Effects of inorganic carbon and pH on growth kinetics of Synechocystis sp. PCC 6803. Algal. Res. 19, 363–369.
Nguyen, B.T., Rittmann, B.E., 2016b. Electron partitioning in soluble organic products by wild-type and modified Synechocystis sp. PCC 6803. Biomass Bioenergy 90, 237–242.
Nguyen, B.T., Rittmann, B.E., 2015. Predicting dissolved inorganic carbon in photoautotrophic microalgae culture via the nitrogen source. Environ. Sci. Technol. 49 (16), 9826–9831.
Novikoff, A.B., Hecht, L., Podber, E., Ryan, J., 1952. Phosphatases of rat liver I. The dephosphorylation of adenosinetriphosphate. J. Biol. Chem. 194 (1), 153–170.
Ramesh, A., Lee, D.-J., Hong, S.G., 2006. Soluble microbial products (SMP) and soluble extracellular polymeric substances (EPS) from wastewater sludge. Appl. Microbiol. Biot. 73 (1), 219–225.
Rippka, R., Deruelles, J., Waterbury, J.B., Herdman, M., Stanier, R.Y., 1979. Generic assignments, strain histories and properties of pure cultures of cyanobacteria. Microbiology 111 (1), 1–61.
Rittmann, B.E., 2008. Opportunities for renewable bioenergy using microorganisms. Biotechnol. Bioeng. 100 (2), 203–212.
Rittmann, B.E., Hausner, M., Loffler, F., Love, N.G., Muyzer, G., Okabe, S., Oerther, D.B., Peccia, J., Raskin, L., Wagner, M., 2006. A vista for microbial ecology and environmental biotechnology. Environ. Sci. Technol. 40 (4), 1096–1103.
Rittmann, B.E., McCarty, P.L., 2001. Environmental Biotechnology: Principles and Applications. McGrawHill, New York, p. 400.
Rivkin, R.B., Swift, E., 1985. Phosphorus metabolism of oceanic dinoflagellates: phosphate uptake, chemical composition and growth of Pyrocystis noctiluca. Mar. Biol. 88 (2), 189–198.
Sañudo-Wilhelmy, S.A., Tovar-Sanchez, A., Fu, F.-X., Capone, D.G., Carpenter, E.J., Hutchins, D.A., 2004. The impact of surface-adsorbed phosphorus on phytoplankton Redfield stoichiometry. Nature 432 (7019), 897–901.
Theodorou, M.E., Elrifi, I.R., Turpin, D.H., Plaxton, W.C., 1991. Effects of phosphorus limitation on respiratory metabolism in the green alga Selenastrum minutum. Plant. Physiol. 95 (4), 1089–1095.
Wang, Y., Gan, N., Zhou, Y., Li, T., Cao, Y., Chen, Y., 2017. Novel single-stranded DNA binding protein-assisted fluorescence aptamer switch based on FRET for homogeneous detection of antibiotics. Biosens. Bioelectron. 87, 508–513.
Wingender, J., Neu, T.R., Flemming, H.-C., 1999. What are bacterial extracellular polymeric substances?. In: Microbial Extracellular Polymeric Substances. Springer, pp. 1–19.
Yao, B., Xi, B., Hu, C., Huo, S., Su, J., Liu, H., 2011. A model and experimental study of phosphate uptake kinetics in algae: considering surface adsorption and P-stress. J. Environ. Sci. 23 (2), 189–198.
Youngburg, G.E., Youngburg, M.V., 1930. Phosphorus metabolism. J. Lab. Clin. Med. 16 (2), 158–166.
Zevin, A.S., Nam, T., Rittmann, B., Krajmalnik-Brown, R., 2015. Effects of phosphate limitation on soluble microbial products and microbial community structure in semi-continuous Synechocystis-based photobioreactors. Biotechnol. Bioeng. 112 (9), 1761–1769.
Zhang, H.-L., Fang, W., Wang, Y.-P., Sheng, G.-P., Zeng, R.J., Li, W.-W., Yu, H.-Q., 2013. Phosphorus removal in an enhanced biological phosphorus removal process: roles of extracellular polymeric substances. Environ. Sci. Technol. 47 (20), 11482–11489.
Zhang, Z., Zhou, Y., Zhang, J., Xia, S., 2014. Copper (II) adsorption by the extracellular polymeric substance extracted from waste activated sludge after short-time aerobic digestion. Environ. Sci. Pollut. R. 21 (3), 2132–2140.
Zhou, Y., Nguyen, B.T., Lai, Y.S., Zhou, C., Xia, S., Rittmann, B.E., 2016a. Using flow cytometry to evaluate thermal extraction of EPS from Synechocystis sp. PCC 6803. Algal. Res. 20, 276–281.
Zhou, Y., Xia, S., Zhang, J., Zhang, Z., Hermanowicz, S.W., 2016b. Adsorption characterizations of biosorbent extracted from waste activated sludge for Pb (II) and Zn (II). Desalin. Water. Treat. 57 (20), 9343–9353.
Zhou, Y., Zhang, J., Zhang, Z., Zhou, C., Lai, Y.S., Xia, S., 2017. Enhanced performance of short-time aerobic digestion for waste activated sludge under the presence of cocoamidopropyl betaine. Chem. Eng. J. 320, 494–500.